Earthq Eng & Eng Vib (2019) 18: 159-170 **DOI**: https://doi.org/10.1007/s11803-019-0496-7

# Evaluating the inelastic displacement ratios of moment-resisting steel frames designed according to the Egyptian code

Hamdy Abou-Elfath†

*Structural Engineering Department, Faculty of Engineering, Alexandria University, Alexandria 21544, Egypt*

**Abstract:** Seismic codes estimate the maximum displacements of building structures under the design-basis earthquakes by amplifying the elastic displacements under the reduced seismic design forces with a deflection amplification factor (DAF). The value of DAF is often estimated as $\rho \times R$, where $R$ is the force reduction factor and $\rho$ is the inelastic displacement ratio that accounts for the inelastic action of the structure according to the definition presented by FEMA P695. The purpose of this study is to estimate the $\rho$-ratio of moment resisting steel frames (MRSFs) designed according to the Egyptian code. This is achieved by conducting a series of elastic and inelastic time-history analyses by two sets of earthquakes on four MRSFs designed according to the Egyptian code and having 2, 4, 8 and 12 stories. The earthquakes are scaled to produce maximum story drift ratios (MSDRs) of 1.0%, 1.5%, 2.0% and 2.5%. The mean values of the ρ-ratio are calculated based on the displacement responses of the investigated frames. The results obtained in this study indicate that the consideration of ρ for both the roof drift ratios (RDRs) and the MSDRs equal to 1.0 is a reasonable estimation for MRSFs designed according to the Egyptian code.

**Keywords:** steel frame; story drift; inelastic analysis; earthquake; deflection amplification factor

## 1 Introduction

Estimating the maximum lateral displacement of structures under earthquake loading is considered to be widely important for seismic design. During strong earthquake, large lateral forces are experienced by structures; this in turn causes lateral displacements to take place. The lateral displacements should be controlled to limit possible damage to structural and non-structural components and also to avoid pounding between adjacent structures.

Seismic design codes estimate the maximum displacements under the design-basis earthquakes by amplifying the elastic displacements under the reduced seismic design forces with a deflection amplification factor (DAF). The value of DAF is often estimated as $\rho \times R$, where $R$ is the force reduction factor and $\rho$ is the inelastic displacement ratio that accounts for the inelastic action of the structure during earthquake events. The value of the $\rho$-ratio specified by the European code (Euro code 8, 2004) and the Canadian code (NBCC, 2010) is equal to 1.0, while it equals to 0.7 in the Egyptian code (ECP-201, 2012). The ASCE 7-10 specification (ASCE 7-10, 2010) assigns different values to $\rho$ depending on the type of the structural system. For moment resisting steel frames, the value of $\rho$ specified by the ASCE 7-10 is equal to 0.6875.

Various research works conducted since the 1960s on the single degree of freedom (SDOF) level (e.g., Veletsos and Newmark, 1960; Miranda and Bertero, 1994; Miranda, 2001; Zhai *et al*., 2007; Durucan and Gümüş, 2018) have indicated that the maximum inelastic displacement of a SDOF can be approximated by the elastic displacement of the same SDOF under earthquake loading. This phenomenon is often called the equal displacement rule and is considered a reasonable approximation for inelastic seismic displacements of SDOF systems except for short period systems for which it is non-conservative.

Analytical studies were conducted to evaluate ρ-ratio on the multi-degrees of freedom level. According to the definition presented by FEMA P695 (2009) and by various researchers, the ρ-ratio is determined as the ratio of inelastic to elastic displacements of the multi-story structures under the effect of earthquake loading. Uang and Maarouf (1994) calculated the $\rho$-ratio (DAF/R) for 2- and 13-story steel buildings and 6- and 10-story RC buildings under a set of 8 real earthquakes. They concluded that the value of $\rho$ ranges from 0.7 to 0.9 for estimating the roof drift ratio (RDR), while it is much

**Correspondence to**: Hamdy Abou-Elfath, Structural Engineering Department, Faculty of Engineering, Alexandria University, Alexandria 21544, Egypt
Tel: +20-1001038402
E-mail: hamdyabou@yahoo.com
†Associate Professor

**Received** June 10, 2017; **Accepted** October 23, 2017

higher than 1.0 when estimating the maximum story drift ratio (MSDR). For ductile frame system with stiffness degradation and weak first story, values of $\rho$ as high as 2.0 were observed.

Mahmoudi and Zaree (2013) evaluated the ρ-ratio of conventional concentrically braced frames and buckling-restrained braced frames. They analyzed prototype buildings with single and double bracing bays and with different number of stories and brace configurations. They concluded that the value of $\rho$ ranges from 1.0 to 1.12 for concentrically braced frames and from 1.0 to 1.4 for buckling-restrained braced frames.

Kuşyılmaz and Topkaya (2015) evaluated the displacement amplification factor given by the ASCE 7-10 for steel eccentrically braced frames. Various designs were considered by changing the number of stories, the bay width, the link-length to bay-width ratio, and the seismic hazard intensity. All designs were analyzed using elastic and inelastic time-history analyzes. Their results indicated that the displacement amplification factor given by the ASCE 7-10 provides unconservative estimates of the story drifts.

Samimifar *et al*. (2015) evaluated global and local seismic displacements of RC frames through the inelastic displacement ratio $\rho$. They concluded that the value of $\rho$, which is calculated based on the ratio of maximum inelastic to elastic floor displacements for intermediate RC frames, is equal to 1.0. They also concluded that the $\rho$-ratio calculated based on inelastic story drifts was 20% higher than that of the inelastic floor displacements. They attributed this trend to damage concentration in some specific stories of the RC frames.

The purpose of this study is to evaluate the ρ-ratio for moment resisting steel frames (MRSFs) designed according to the Egyptian code. Four MRSFs having 2, 4, 8 and 12 stories are designed and are analyzed under the effect of two sets of ground motion records. The first set consists of ten American earthquakes; while the second set consist of seven European records compatible in their average with the design response spectrum. The ground motion records are scaled to produce MSDRs of 1.0%, 1.5%, 2.0% and 2.5%. The mean values of the ρ-ratio are calculated based on the ratios of inelastic to elastic displacements of the multi-story frames.

## 2 Design of buildings

Four steel office buildings having 2, 4, 8 and 12 stories representing a wide range of MRSF heights are considered in this study. The four buildings have the same floor plan shown in Fig. 1, which has a rectangular configuration with 5-bays in the long direction and 3- bays in the short direction. The bay width is constant and equals to 7.5 m, while the story height is considered 4.5 m for the first story and 3.5 m for the upper stories. Lateral resisting of the buildings is assumed to be provided by perimeter MRSFs in the short direction and perimeter braced steel frames in the long direction. The perimeter MRSFs of the four buildings are shown in Figs. 2-5.

The building floors are assumed to be consisting of metal deck with normal weight concrete topping. The dead load is estimated as 5 kPa and it includes weights of deck, beams, girders, ceiling, partitions and mechanical and electrical systems. Weight of the exterior walls is considered equal to 1.25 kPa of surface. The applied live load considered is taken 2.5 kPa for office buildings. The buildings are assumed to be located in Cairo, Egypt (seismic zone 3) with a design ground acceleration of 0.15 g which is associated with 10% probability of exceedance in 50 years. Soil type 'C' and suburban exposure conditions are considered in lateral load calculations. The frames are considered to have adequate-ductility with $R$-factor equal to 7. Steel members are selected from the standard American wide flange W-sections with the ASTM A992 specification ($F_y$ = 345 MPa). Modulus of elasticity of steel is considered 200 GPa and the strain hardening ratio is 0.01. The non-structural elements are assumed to be fully isolated from the structure deformations. The story drift limit specified by the ECP-201 provisions is equal to 1.0% at the serviceability earthquake intensity which is equivalent to 2.0% at the design basis earthquake intensity.

The frames are first designed using the gravity and the lateral loads specified by the code and then the lateral drifts are checked and found higher than the limits specified by the ECP-201 provisions. Satisfying the lateral drift conditions requires increasing the lateral stiffness of the frames by increasing the sizes of the cross sections. However, this process of increasing

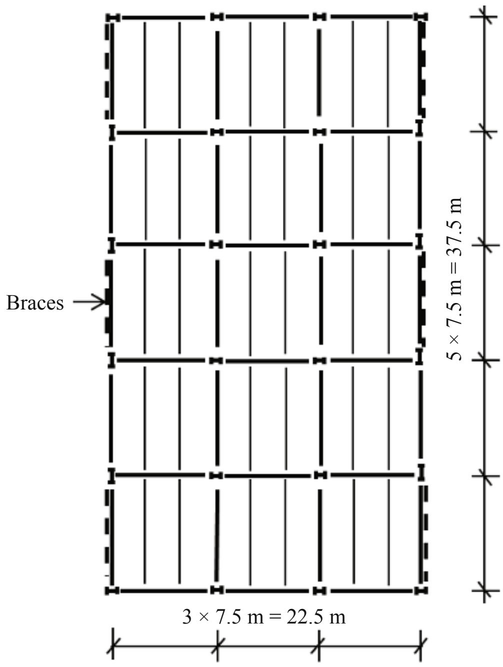


**Fig. 1 Floor plan of the two, four, eight and twelve-story buildings**

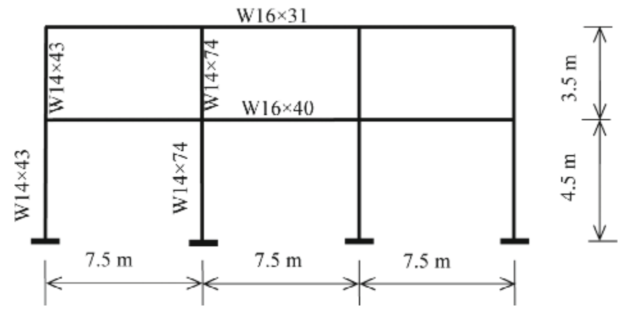


**Fig. 2 Design details of the two-story MRSF**

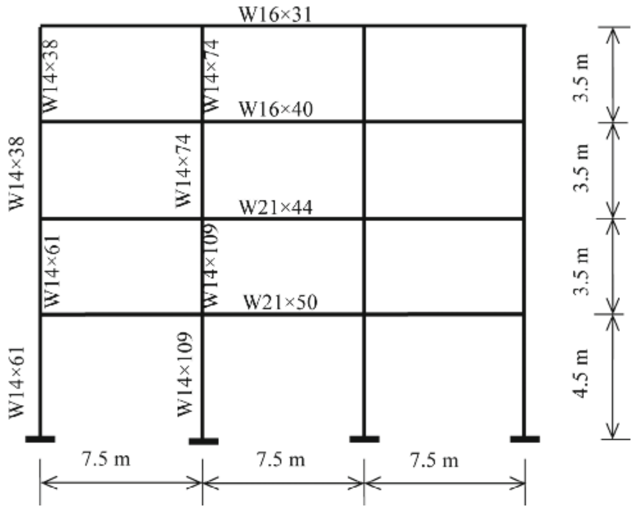


**Fig. 3 Design details of the four-story MRSF**

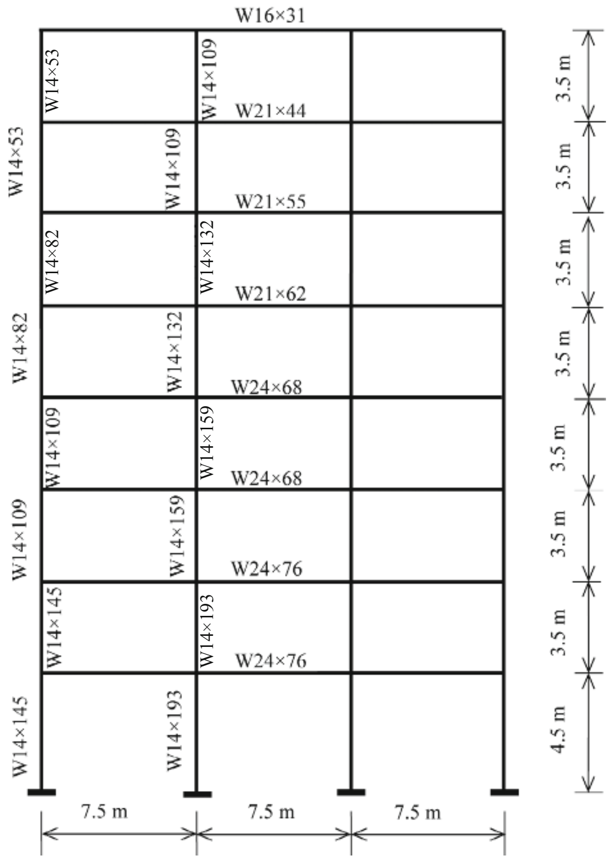


**Fig. 4 Design details of the eight-story MRSF**

the sizes of the cross sections require maintaining the relative stiffnesses of the various stories obtained by the strength-based design along with maintaining the relative strengths of beams and columns at each joint to ensure the strong-column weak beam behavior. In the current study, the drift design is accomplished by gradually increasing the design lateral forces while keeping their distribution unchanged and repeating the strength-based design until satisfying the lateral drift requirements. By this approach, the relative strengths of beams and columns at each joint and the relative stiffnesses of the frame stories are maintained while the drift conditions are accomplished. The column sections are allowed to be changed every two stories. The design details of the four MRSFs are shown in Figs. 2-5.

The maximum story drift ratios due to the design lateral loading ($MSDR_0$) are summarized in Table 1. The amplified story drift ratios at the design-basis and the serviceability earthquake limits ($MSDR_1$ and $MSDR_2$, respectively) are also summarized in the table. The results summarized in Table 1 are slightly lower than the design levels because the column sections are allowed to be changed every two stories.

The fundamental periods of the four frames are presented in Table 2. The fundamental periods of the frames calculated by the ECP-201 empirical equation ($T$ = 0.085 $H^{3/4}$, where $H$ is the frame height) are also presented in the table. It can be observed that the actual fundamental periods of the frames are much longer than the values suggested by the ECP-201 empirical equation. The calculated periods of the designed structures can be

**Table 1 Lateral deformations of the design cases calculated based on the design lateral loading**

| Design case | Design base shear coefficient (%) | $MSDR_0$ (%) | (Design-basis level) $MSDR_1 = 0.7R\times MSDR_0$ (%) | (Serviceability level) $MSDR_2 = 0.5\times MSDR_1$ (%) |
|---|---|---|---|---|
| 2-story | 0.05 | 0.39 | 1.91 | 0.96 |
| 4-story | 0.31 | 0.39 | 1.91 | 0.96 |
| 8-story | 0.03 | 0.40 | 1.96 | 0.98 |
| 12-story | 0.03 | 0.37 | 1.81 | 0.91 |

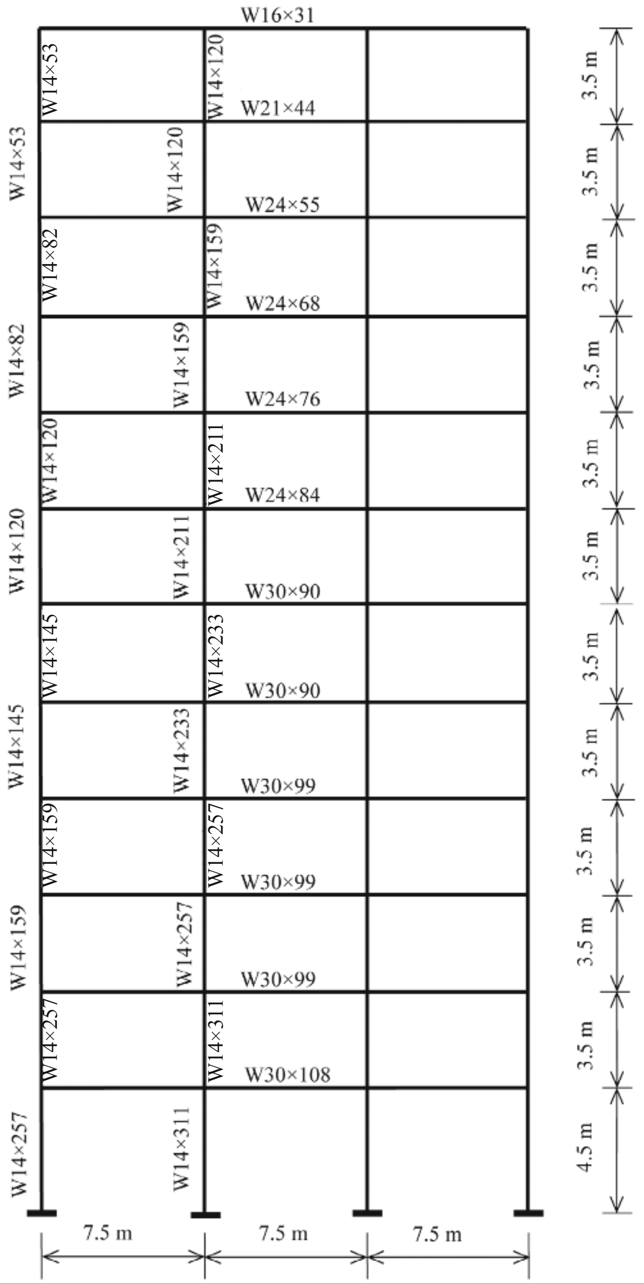


**Fig. 5 Design details of the twelve-story MRSF**

justified because of the following reasons:

(1) The period equations are usually calibrated with buildings located in high seismicity regions. These buildings are designed using high levels of lateral loading and are expected to have higher stiffness and shorter periods than structures designed in low or moderate seismicity zones.

(2) The effect of nonstructural components and gravity-only columns and beams is ignored in the current analysis.

(3) The code equation is expected to yield shorter periods than the actual values to provide safety margins to the designed buildings.

**Table 2 Fundamental periods of the MRSFs**

| Case | Period | |
|---|---|---|
| | Design | Actual |
| 2-story | 0.404 | 1.357 |
| 4-story | 0.648 | 2.096 |
| 8-story | 1.062 | 2.838 |
| 12-story | 1.427 | 3.209 |

## 3 Structural modeling and assumptions

The MRSFs are analytically modeled using the SeismoStruct computer program (SeismoStruct v7.0, 2014). Beams and columns are represented by the force-based beam-column element that utilizes the fiber modeling approach which relies on using a number of control sections along the element length and subdividing the control sections into steel fibers to capture the spread of inelasticity along the cross sections and the member length. A uniaxial bilinear stress-strain model with kinematic strain hardening is assigned for each fiber. A simplified loading and reloading rules without strength and the stiffness deterioration are considered for hysteretic modeling. The sectional stress-strain state is obtained through the integration of the nonlinear uniaxial stress-strain response of the individual fibers forming the cross-section while the member response is obtained by integrating the responses of the control sections along the member length.

Centerline dimensions are considered in modeling the frame members to account approximately for the flexibility of the panel zones. The seismic mass is considered equal to the dead load plus half of the live load and is considered lumped at the frame joints only. Each MRSF in the short direction is assigned half of the building mass to simulate the actual behavior of the structure during the earthquake application. The contribution of the gravity-only beams and columns in resisting lateral loads is ignored as it has little effect on the overall lateral resistance of the building. The effect of the geometric non-linearity ($P$-$\Delta$ effect) is considered in the analysis. Time-history analysis is performed using a Rayleigh damping which is defined to achieve 5.0% viscous damping in the first two natural modes of the frames.

## 4 The Inelastic displacement ratio

Figure 6 shows global inelastic response of a structure under the effect of lateral loading. The actual inelastic response is idealized by a bilinear relation between the base shear and a lateral displacement component of the structure. $F_d$ and $\Delta_d$ are the design base shear and displacement, respectively, while $F_e$ and $\Delta_e$ are the base shear and the displacement demands calculated using

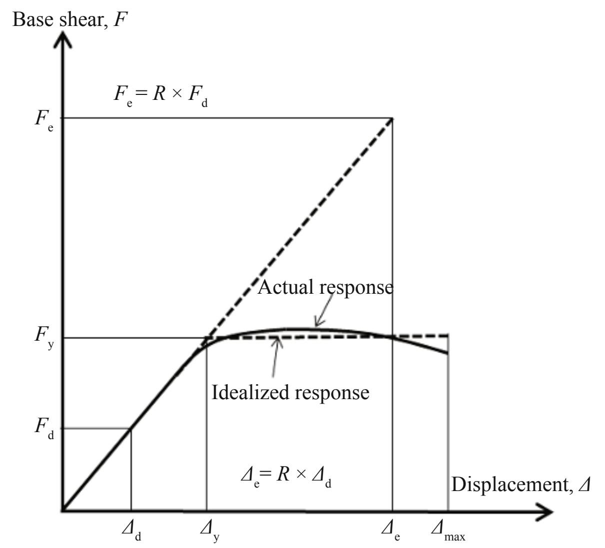


**Fig. 6 General structural response under the effect of lateral loading**

linear-elastic earthquake analysis, respectively. $\Delta_{max}$ represents the maximum displacement demands under inelastic earthquake analysis. The elastic force and displacement demands $F_e$ and $\Delta_e$ are related to the design force and displacement demands $F_d$ and $\Delta_d$ according to the following relation:

$$\frac{F_e}{F_d} = \frac{\Delta_e}{\Delta_d} = R \tag{1}$$

According to the definition presented by FEMA P695 (2009) and by various researchers such as Uang and Maarouf (1994), the inelastic displacement ratio ρ is calculated according to the following equation.

$$\rho = \frac{DAF}{R} = \frac{(\Delta_{max} / \Delta_d)}{R} = \frac{\Delta_{max}}{\Delta_e} \tag{2}$$

This indicates that the inelastic displacement ratio $\rho$ is equal to the ratio of inelastic to elastic displacements of the multi-story structures under the effect of earthquake loading. The ratio is dependent on the displacement component to be considered in the calculations. In the current study, the inelastic ratio $\rho$ is estimated for the RDRs and the MSDRs.

## 5 Pushover responses

The MRSFs considered in this study are subjected to pushover loading. The pushover loading is carried out by applying a static lateral load having the distribution pattern specified in the Egyptian code ECP-201 which can be expressed as:

$$F_i = V \frac{w_i h_i}{\sum_{j=1}^{n} w_j h_j} \tag{3}$$

where, $F_i$ is the concentrated force at level $i$, $V$ is the base shear, $w_i$ is the lumped seismic weight of level $i$, $h_i$ is the height of level $i$ from the ground, and $n$ is the number of stories. For equal floor masses and equal story heights the distribution shape given by the code formula is an inverted triangle which is a reasonable approximation of the first mode response.

A displacement controlled analysis is conducted until the structure reaches a 2.5% MSDR. The results of the pushover analysis obtained provide information on the structure lateral strength and stiffness. The distributions of the story displacements along the height obtained from the pushover analysis are very important in evaluating the overall ductility of the structure.

Figure 7 shows the relationships between the base shear coefficients and the MSDRs of the frames. The design base shear coefficients of the 2-, 4-, 8- and 12-story frames are 0.05, 0.031, 0.03 and 0.03, respectively. The design lateral forces of the 8- and the 12-story frames are governed by the lower limit on the base shear imposed by the code to provide strength and safety for long period structures. The results shown in Fig. 7 indicate that the 4-, 8- and 12-story frames have comparable lateral strength and initial stiffnesses because they have similar design base-shears and drift limits.

Figures 8(a)-(d) show the height-wise distribution of story drifts for the four frames considered in this study at 2.5% MSDR. The results shown in the figures indicate that the MSDRs occurred in the first story of the 2- and the 4-story frames and in the third story of the 8- and the 12-story frames.

The over-strength factor is defined in this study as the yield base shear divided by the design base-shear. The yield base shear is approximately estimated as the

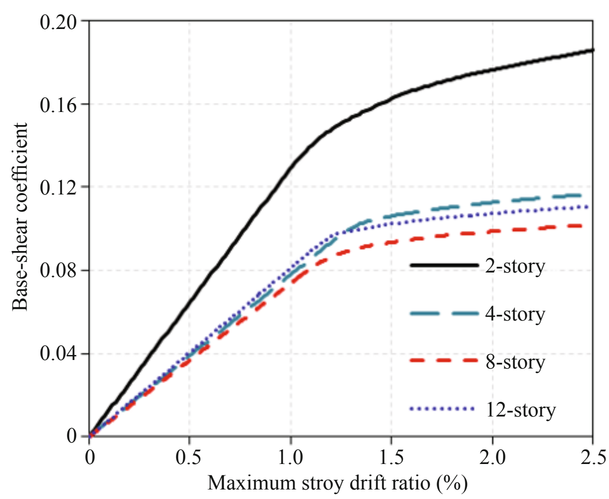


**Fig. 7 Relationships between the base-shear coefficient and the MSDR**

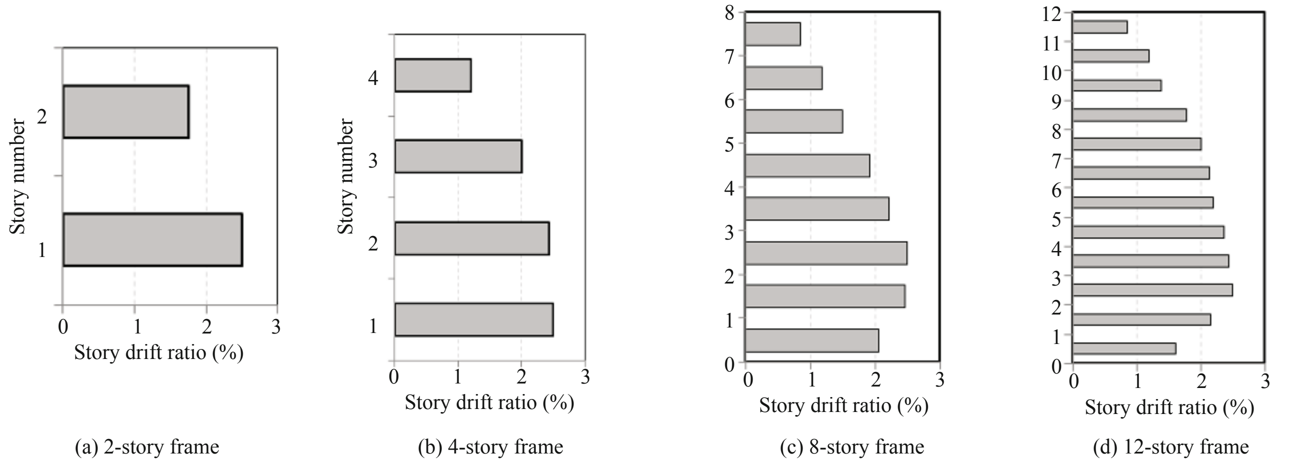


**Fig. 8 Height-wise distribution of the story drift ratios at 2.5% MSDR**

**Table 3 Over-strength factors of the four frames**

| Design case | Over-strength factor |
|---|---|
| 2-story | 3.02 |
| 4-story | 3.12 |
| 8-story | 2.93 |
| 12-story | 3.27 |

base-shear that corresponds to 1.25% maximum story drift ratio. For the 2-, 4-, 8- and 12 story frames, the yield base shear coefficients are 0.151, 0.097, 0.088 and 0.098, respectively. The design base shear coefficients are 0.05, 0.031, 0.03 and 0.03 for the 2-, 4-, 8- and 12 story frames, respectively. Table 3 summarizes the over-strength factors of the four frames designed in this study.

## 6 Seismic performances

The frames are subjected to two sets of ground motions. The first set consists of ten American earthquakes that cover a wide range of frequency contents and durations. The records are selected from the 1979 Imperial Valley, 1987 Superstition Hills, and the 1989 Loma Prieta earthquakes (COSMOS, 2017). The Earthquake data and site information are summarized in Table 4 and the response spectra of the selected records are shown in Figs. 9(a) and (b).

The earthquake response of the four frames considered in this study is calculated using the SeismoStruct computer program. Gravity loads are applied on the frame during the earthquake analysis and are considered equal to the dead loads plus half of the live loads. The selected earthquakes are scaled to produce MSDRs of 1%, 1.5%, 2% and 2.5%. Earthquake analysis of the frames is performed twice, once with considering the frame material behaves elastically and once with considering the inelastic effect. The mean PGA levels considered in the analysis of the four frames to produce the specified MSDRs are summarized in Table 5. The ρ-ratio calculated for the RDR and the MSDR of the MRSFs due to earthquake loading are presented in Tables 6 to 9 at 1%, 1.5%, 2% and 2.5% MSDRs, respectively.

**Table 4 Earthquake data and site information for the selected ground motions**

| Record No | Event | Year | Record Station | $\Phi$ | $M$ | $R$ (km) | PGA (g) |
|---|---|---|---|---|---|---|---|
| 1 | Loma Prieta | 1989 | Anderson Dam | 270 | 6.9 | 21.4 | 0.244 |
| 2 | Imperial Valley | 1979 | El Centro Array # 13 | 230 | 6.5 | 21.9 | 0.139 |
| 3 | Imperial Valley | 1979 | Chihuahua | 282 | 6.5 | 28.7 | 0.254 |
| 4 | Imperial Valley | 1979 | Cucapah | 85 | 6.9 | 23.6 | 0.309 |
| 5 | Imperial Valley | 1979 | El Centro Array # 13 | 140 | 6.5 | 21.9 | 0.117 |
| 6 | Loma Prieta | 1989 | Holister South & Pine | 0 | 6.9 | 28.8 | 0.371 |
| 7 | Loma Prieta | 1989 | Sunnyvale Colton Ave | 360 | 6.9 | 28.8 | 0.209 |
| 8 | Loma Prieta | 1989 | Waho | 90 | 6.9 | 16.9 | 0.638 |
| 9 | Superstition Hill | 1987 | Wildlife Liquefaction Array | 90 | 6.5 | 24.4 | 0.18 |
| 10 | Superstition Hill | 1987 | Wildlife Liquefaction Array | 360 | 6.7 | 24.4 | 0.2 |

$\Phi$ is the component, $M$ is the magnitude, $R$ is the epicenter distance, PGA is the peak ground acceleration

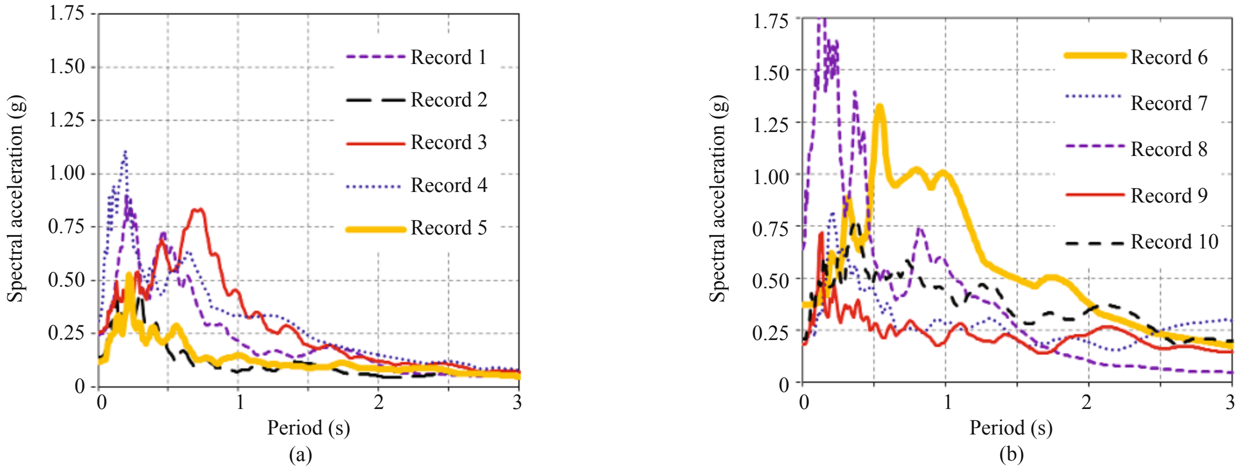


**Fig. 9 Spectral accelerations of the selected earthquake records**

**Table 5 The mean PGAs in g required to produce the specified MSDRs**

| Design case | MSDR | | | |
|---|---|---|---|---|
| | 1.0% | 1.5% | 2.0% | 2.5% |
| 2-story | 0.15 | 0.22 | 0.32 | 0.40 |
| 4-story | 0.18 | 0.26 | 0.35 | 0.46 |
| 8-story | 0.20 | 0.31 | 0.42 | 0.54 |
| 12-story | 0.21 | 0.31 | 0.41 | 0.52 |

The relationships between the number of stories and the mean values of the $\rho$-ratio calculated for the RDR and the MSDR are shown in Figs. 10 and 11, respectively. The results shown in Figs. 10 and 11 indicate that the upper limit of the mean $\rho$-ratios for both the RDR and the MSDR is nearly 1.0 and that the mean values of the $\rho$-ratios for both the RDR and the MSDR decrease with the increase in the experienced MSDRs of the frames. The results also indicate that the mean $\rho$-ratios of the MSDR tend to increase with the increase in the number of stories.

The MSDRs experienced by the four frames considered in this study under the effect of the ten selected ground motion records when scaled to PGA level of 0.15 g are presented in Table 10. The level of 0.15 g represents the design PGA of the frames. The mean values of the MSDRs presented in Table 10 indicate that the four frames experience low levels of inelastic deformations at the design PGA. This can be attributed to the over-strength provided to these frames to satisfy the drift limits specified by the code and also because of the high levels of the actual periods of the frames in comparison with the estimated periods by the code equation. Due to the expected low levels of inelastic deformations in MRSFs designed according to the Egyptian code, the consideration of $\rho$ for both the RDR and the MSDR equal to 1.0 is a reasonable estimation.

The earthquake responses of the four frames considered in this study are also calculated under the

**Table 6 Inelastic displacement ratios at 1.0% MSDR**

| Record No. | 2-story frame | | 4-story frame | | 8-story frame | | 12-story frame | |
|---|---|---|---|---|---|---|---|---|
| | RDR | MSDR | RDR | MSDR | RDR | MSDR | RDR | MSDR |
| 1 | 1.000 | 1.000 | 1.000 | 1.000 | 1.000 | 1.000 | 1.000 | 1.000 |
| 2 | 0.997 | 1.000 | 1.002 | 1.000 | 1.000 | 1.000 | 1.000 | 1.000 |
| 3 | 1.000 | 1.000 | 1.000 | 1.000 | 1.000 | 1.000 | 1.000 | 1.000 |
| 4 | 1.000 | 1.000 | 1.000 | 1.000 | 1.000 | 1.000 | 1.000 | 1.000 |
| 5 | 1.000 | 1.000 | 1.000 | 1.000 | 0.999 | 1.000 | 1.000 | 1.000 |
| 6 | 1.000 | 1.000 | 1.000 | 1.000 | 1.000 | 1.000 | 1.000 | 1.000 |
| 7 | 0.996 | 0.997 | 1.000 | 1.000 | 1.000 | 1.000 | 1.000 | 1.000 |
| 8 | 0.999 | 0.997 | 1.000 | 1.000 | 1.000 | 1.000 | 1.000 | 1.000 |
| 9 | 1.000 | 1.000 | 1.000 | 1.000 | 1.000 | 1.000 | 1.000 | 1.000 |
| 10 | 1.000 | 1.000 | 1.000 | 1.000 | 1.000 | 1.000 | 1.000 | 1.000 |
| Mean | 0.999 | 0.999 | 1.000 | 1.000 | 1.000 | 1.000 | 1.000 | 1.000 |

**Table 7 Inelastic displacement ratios at 1.5% MSDR**

| Record No. | 2-story frame | | 4-story frame | | 8-story frame | | 12-story frame | |
|---|---|---|---|---|---|---|---|---|
| | RDR | MSDR | RDR | MSDR | RDR | MSDR | RDR | MSDR |
| 1 | 0.985 | 1.040 | 1.093 | 0.963 | 0.988 | 0.954 | 0.986 | 0.972 |
| 2 | 0.898 | 1.002 | 1.078 | 1.145 | 0.868 | 0.916 | 0.985 | 1.033 |
| 3 | 0.855 | 0.908 | 1.000 | 1.000 | 0.988 | 0.990 | 0.998 | 1.019 |
| 4 | 0.810 | 0.913 | 1.000 | 1.000 | 1.002 | 1.010 | 0.997 | 1.017 |
| 5 | 0.904 | 0.928 | 0.930 | 0.980 | 0.962 | 0.866 | 0.986 | 1.018 |
| 6 | 0.889 | 0.915 | 0.945 | 0.929 | 1.000 | 1.028 | 1.000 | 1.019 |
| 7 | 0.981 | 1.042 | 0.994 | 0.965 | 0.851 | 0.922 | 0.967 | 1.020 |
| 8 | 0.913 | 0.994 | 1.000 | 1.000 | 0.987 | 1.010 | 0.999 | 1.012 |
| 9 | 0.927 | 0.992 | 0.937 | 0.890 | 0.951 | 1.009 | 0.951 | 1.004 |
| 10 | 0.974 | 1.036 | 0.983 | 0.975 | 0.874 | 0.906 | 0.933 | 0.917 |
| Mean | 0.913 | 0.977 | 0.996 | 0.985 | 0.947 | 0.961 | 0.980 | 1.003 |

**Table 8 Inelastic displacement ratios at 2.0% MSDR**

| Record No. | 2-story frame | | 4-story frame | | 8-story frame | | 12-story frame | |
|---|---|---|---|---|---|---|---|---|
| | RDR | MSDR | RDR | MSDR | RDR | MSDR | RDR | MSDR |
| 1 | 0.752 | 0.835 | 0.920 | 0.865 | 0.864 | 0.887 | 0.971 | 0.978 |
| 2 | 0.737 | 0.879 | 1.035 | 1.251 | 0.791 | 0.894 | 0.899 | 0.986 |
| 3 | 0.818 | 0.923 | 1.004 | 1.034 | 0.939 | 1.014 | 0.990 | 1.140 |
| 4 | 0.816 | 0.977 | 1.016 | 1.030 | 1.019 | 1.046 | 0.984 | 1.070 |
| 5 | 0.710 | 0.841 | 0.903 | 0.944 | 0.738 | 0.717 | 0.852 | 0.889 |
| 6 | 0.807 | 0.909 | 0.873 | 0.911 | 1.001 | 1.076 | 1.000 | 1.078 |
| 7 | 0.973 | 1.100 | 0.859 | 0.988 | 0.584 | 0.675 | 0.823 | 0.936 |
| 8 | 0.850 | 0.906 | 1.001 | 1.025 | 0.989 | 1.072 | 0.982 | 1.061 |
| 9 | 0.970 | 1.091 | 0.937 | 0.944 | 0.886 | 1.072 | 0.849 | 1.047 |
| 10 | 0.792 | 0.913 | 0.722 | 0.769 | 0.867 | 0.966 | 0.841 | 0.909 |
| Mean | 0.823 | 0.937 | 0.927 | 0.976 | 0.868 | 0.942 | 0.919 | 1.009 |

**Table 9 Inelastic displacement ratios at 2.5% MSDR**

| Record No. | 2-story frame | | 4-story frame | | 8-story frame | | 12-story frame | |
|---|---|---|---|---|---|---|---|---|
| | RDR | MSDR | RDR | MSDR | RDR | MSDR | RDR | MSDR |
| 1 | 0.792 | 0.907 | 0.740 | 0.793 | 0.649 | 0.881 | 0.919 | 0.969 |
| 2 | 0.761 | 0.931 | 0.834 | 1.067 | 0.770 | 0.892 | 0.762 | 0.810 |
| 3 | 0.847 | 0.984 | 1.012 | 1.114 | 0.828 | 1.031 | 0.974 | 1.228 |
| 4 | 0.834 | 1.033 | 0.973 | 1.027 | 1.039 | 0.990 | 0.958 | 1.097 |
| 5 | 0.681 | 0.759 | 0.899 | 0.991 | 0.683 | 0.710 | 0.695 | 0.887 |
| 6 | 0.613 | 0.719 | 0.888 | 0.947 | 1.003 | 1.025 | 1.000 | 1.093 |
| 7 | 0.895 | 1.062 | 0.920 | 1.128 | 0.496 | 0.655 | 0.639 | 0.704 |
| 8 | 0.793 | 0.869 | 0.929 | 1.008 | 0.981 | 1.118 | 0.967 | 1.159 |
| 9 | 1.042 | 1.198 | 0.887 | 0.950 | 0.899 | 1.127 | 0.882 | 1.101 |
| 10 | 0.677 | 0.760 | 0.538 | 0.534 | 0.669 | 0.821 | 0.727 | 0.922 |
| Mean | 0.793 | 0.922 | 0.862 | 0.956 | 0.802 | 0.925 | 0.852 | 0.997 |

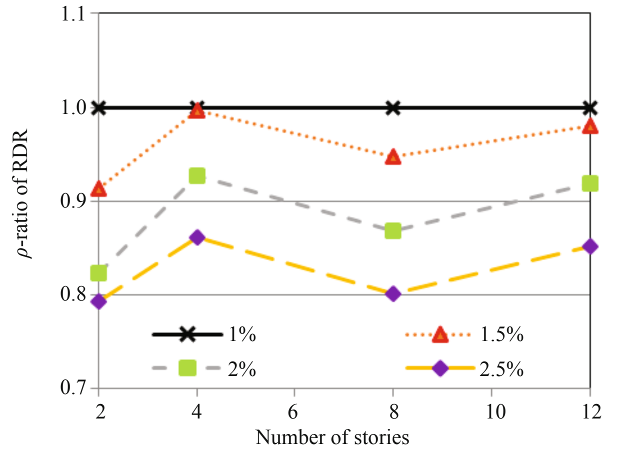


**Fig. 10 Relationships between the number of stories and the *ρ*-ratio of RDRs**

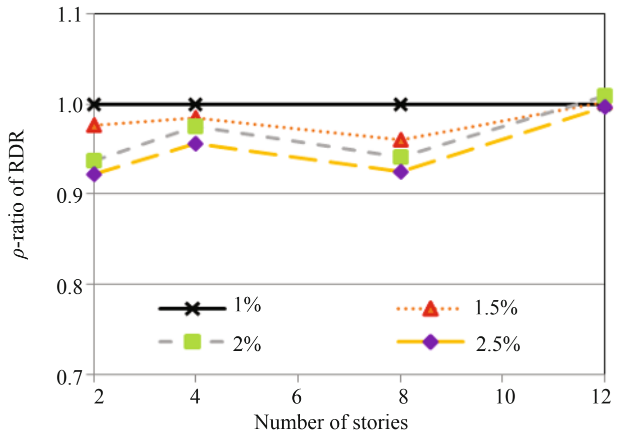


**Fig. 11 Relationships between the number of stories and the *ρ*-ratio of MSDRs**

**Table 10 MSDRs of the four frames at PGA level of 0.15g (%)**

| Record No. | 2-story | 4-story | 8-story | 12-story |
|---|---|---|---|---|
| 1 | 0.674 | 0.651 | 0.462 | 0.476 |
| 2 | 0.844 | 0.490 | 0.608 | 0.486 |
| 3 | 1.179 | 0.945 | 0.831 | 0.830 |
| 4 | 1.059 | 0.810 | 0.648 | 0.700 |
| 5 | 0.938 | 1.109 | 0.845 | 0.764 |
| 6 | 1.428 | 1.541 | 1.362 | 1.186 |
| 7 | 1.585 | 1.339 | 1.815 | 1.997 |
| 8 | 0.619 | 0.337 | 0.352 | 0.352 |
| 9 | 1.137 | 2.361 | 1.420 | 1.192 |
| 10 | 2.042 | 2.080 | 1.521 | 1.501 |
| Mean | 1.150 | 1.166 | 0.986 | 0.948 |

effect of a suit of earthquakes that match the spectral intensity of the design spectrum of zone 3 in the Egyptian code. A software package REXEL v 3.5 beta (Iervolino *et al*., 2010) is employed to search for a set of seven European records compatible in their average with a pre-defined spectrum. The European strong motion database is used for the search because it includes past earthquakes in Egypt. To reflect seismological features of the Cairo region, the search was restricted to records having magnitude between 5 and 6 and to stations located on soft soil conditions (Type C). Characteristics of selected earthquake records according to REXEL search are shown in Table 11. Figure 12 shows the 5% damped spectra of the earthquakes while Fig. 15 shows the code design spectrum and the average spectrum of the selected earthquakes.

The ρ-ratio calculated for the RDR and the MSDR of the MRSFs due to earthquake loading are presented in Tables 12 to 15 at 1%, 1.5%, 2% and 2.5% MSDRs, respectively.

The relationships between the number of stories and the mean values of the ρ-ratio calculated for the RDR and the MSDR are shown in Figs. 14 and 15, respectively. The results shown in the figures indicate that the upper limit of the mean ρ-ratios for both the RDR and the MSDR is 1.0 and that the mean values of the ρ-ratios for both the RDR and the MSDR tend to decrease with the increase in the experienced MSDRs. The results also indicate that the mean *ρ*-ratios of the MSDR tend

**Table 11 Characteristics of the second set of earthquakes**

| Record No. | Earthquake | *M* | *R* (km) | Soil type | PGA (g) |
|---|---|---|---|---|---|
| 1 | Chenoua | 5.9 | 29 | C | 0.345 |
| 2 | NE of Banja Luka | 5.7 | 7 | C | 0.261 |
| 3 | NE of Banja Luka | 5.7 | 7 | C | 0.253 |
| 4 | Sicilia-Orientale | 5.6 | 24 | C | 0.288 |
| 5 | Chenoua | 5.9 | 29 | C | 0.230 |
| 6 | Umbria Marche | 5.7 | 3 | C | 0.222 |
| 7 | Umbria Marche | 5.7 | 3 | C | 0.405 |

*M* is the magnitude, *R* is the epicenter distance and PGA is the peak ground acceleration

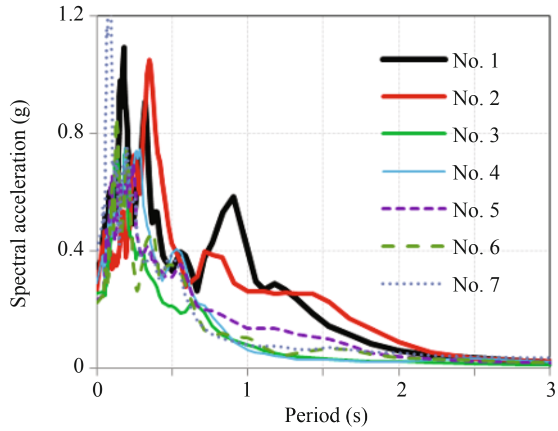


**Fig. 12 5% damped spectra of the earthquakes**

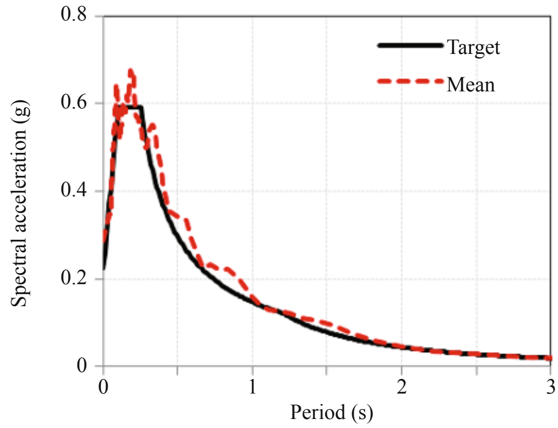


**Fig. 13 Code design spectrum and the average spectrum of the selected earthquakes**

**Table 12 Inelastic displacement ratios at 1.0% MSDR**

| Record No. | 2-story frame | | 4-story frame | | 8-story frame | | 12-story frame | |
|---|---|---|---|---|---|---|---|---|
| | RDR | MSDR | RDR | MSDR | RDR | MSDR | RDR | MSDR |
| 1 | 1.000 | 1.000 | 1.000 | 1.000 | 1.000 | 1.000 | 1.000 | 1.000 |
| 2 | 1.000 | 1.000 | 1.006 | 1.000 | 1.000 | 1.000 | 1.000 | 1.000 |
| 3 | 1.000 | 1.000 | 1.000 | 1.000 | 1.000 | 1.000 | 1.000 | 1.000 |
| 4 | 1.000 | 1.000 | 1.000 | 1.000 | 1.000 | 1.000 | 1.000 | 1.000 |
| 5 | 1.000 | 1.000 | 1.000 | 1.000 | 1.000 | 1.000 | 1.000 | 1.000 |
| 6 | 1.000 | 1.000 | 1.000 | 1.000 | 1.000 | 1.000 | 1.000 | 1.000 |
| 7 | 1.000 | 1.000 | 1.000 | 1.000 | 0.999 | 1.000 | 1.000 | 1.000 |
| Mean | 1.000 | 1.000 | 1.000 | 1.000 | 1.000 | 1.000 | 1.000 | 1.000 |

**Table 13 Inelastic displacement ratios at 1.5% MSDR**

| Record No. | 2-story frame | | 4-story frame | | 8-story frame | | 12-story frame | |
|---|---|---|---|---|---|---|---|---|
| | RDR | MSDR | RDR | MSDR | RDR | MSDR | RDR | MSDR |
| 1 | 0.826 | 0.827 | 1.000 | 1.003 | 0.973 | 0.995 | 0.991 | 1.014 |
| 2 | 0.778 | 0.775 | 0.999 | 1.000 | 1.000 | 1.006 | 0.987 | 1.007 |
| 3 | 0.934 | 0.956 | 1.006 | 0.977 | 1.011 | 1.003 | 1.001 | 1.005 |
| 4 | 1.073 | 0.993 | 0.975 | 0.987 | 0.759 | 0.775 | 1.000 | 1.003 |
| 5 | 0.989 | 1.017 | 1.000 | 1.000 | 0.976 | 1.001 | 0.966 | 0.988 |
| 6 | 0.878 | 0.831 | 0.981 | 0.986 | 0.998 | 1.017 | 0.945 | 0.969 |
| 7 | 1.000 | 0.999 | 0.88 | 0.918 | 0.894 | 1.004 | 0.969 | 1.01 |
| Mean | 0.925 | 0.914 | 0.977 | 0.982 | 0.944 | 0.972 | 0.98 | 0.999 |

**Table 14 Inelastic displacement ratios at 2.0% MSDR**

| Record No. | 2-story frame | | 4-story frame | | 8-story frame | | 12-story frame | |
|---|---|---|---|---|---|---|---|---|
| | RDR | MSDR | RDR | MSDR | RDR | MSDR | RDR | MSDR |
| 1 | 0.743 | 0.808 | 1.014 | 1.05 | 0.831 | 1.02 | 1.008 | 1.021 |
| 2 | 0.671 | 0.681 | 1 | 1.041 | 1.016 | 1.053 | 0.911 | 0.976 |
| 3 | 0.814 | 0.832 | 0.851 | 0.755 | 0.849 | 0.923 | 1.02 | 0.948 |
| 4 | 1.108 | 0.989 | 0.771 | 0.836 | 0.626 | 0.734 | 1.035 | 0.853 |
| 5 | 0.808 | 0.878 | 0.977 | 0.966 | 1.108 | 0.91 | 0.932 | 1.049 |
| 6 | 0.941 | 0.932 | 0.873 | 0.95 | 0.853 | 0.935 | 0.758 | 0.93 |
| 7 | 1.004 | 1.086 | 0.883 | 0.982 | 0.943 | 1.006 | 0.89 | 1.068 |
| Mean | 0.87 | 0.887 | 0.91 | 0.94 | 0.889 | 0.94 | 0.936 | 0.978 |

**Table 15 Inelastic displacement ratios at 2.5% MSDR**

| Record No. | 2-story frame | | 4-story frame | | 8-story frame | | 12-story frame | |
|---|---|---|---|---|---|---|---|---|
| | RDR | MSDR | RDR | MSDR | RDR | MSDR | RDR | MSDR |
| 1 | 0.646 | 0.737 | 0.971 | 1.083 | 0.838 | 1.059 | 1.095 | 0.882 |
| 2 | 0.681 | 0.712 | 1.025 | 1.112 | 1.16 | 1.099 | 0.914 | 1.007 |
| 3 | 0.813 | 0.857 | 0.639 | 0.635 | 0.796 | 0.948 | 1.086 | 0.908 |
| 4 | 0.967 | 1.027 | 0.826 | 0.65 | 0.458 | 0.602 | 0.915 | 0.622 |
| 5 | 0.62 | 0.692 | 0.934 | 0.742 | 1.436 | 0.84 | 1.057 | 1.052 |
| 6 | 1.002 | 1.009 | 0.716 | 0.859 | 0.626 | 0.677 | 0.657 | 0.998 |
| 7 | 1.041 | 1.194 | 0.922 | 1.05 | 1.011 | 1.054 | 0.916 | 1.095 |
| Mean | 0.824 | 0.89 | 0.862 | 0.876 | 0.904 | 0.897 | 0.949 | 0.938 |

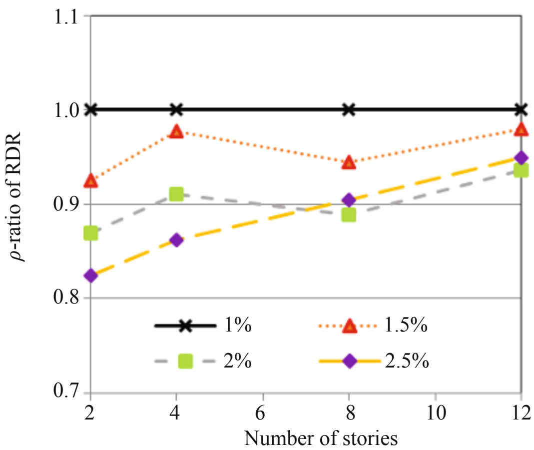


**Fig. 14 Relationships between the number of stories and the $\rho$-ratio of the RDR**

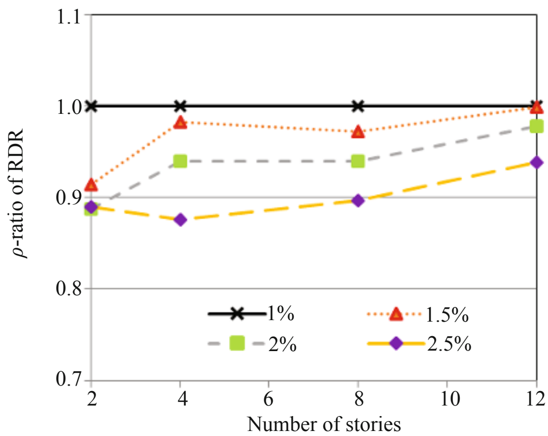


**Fig. 15 Relationships between the number of stories and the $\rho$-ratio of the MSDR**

to increase with the increase in the number of stories. This behavior of the four frames under the second set of earthquakes is identical to the behavior obtained under the effect of the first earthquake set

## 7 Conclusions

(1) The ρ-ratios of moment resisting steel frames designed according to the Egyptian code have been evaluated in this study. Four MRSFs having 2, 4, 8 and 12 stories are designed and are analyzed under the effect of two sets of ground motion records. Based on the results obtained, the following conclusions are drawn.

(2) The upper limit of the mean ρ-ratios calculated for the RDR and the MSDR is nearly equal to 1.0.

(3) The mean $\rho$-ratio calculated for the RDR and the MSDR decreases with the increase in the experienced MSDRs of the frames.

(4) The mean $\rho$-ratio calculated for the MSDR increases with the increase in the number of stories.

(5) The consideration of ρ for both the RDR and the MSDR equals to 1.0 is a reasonable estimation for MRSFs designed according to the Egyptian code because of the expected low levels of inelastic deformations.

The current study assumes 1.0 % allowable story drift limit at the serviceability earthquake intensity which is equivalent to 2.0% at the design basis earthquake intensity. The performance of structures designed with different levels of allowable story drift limits need to be investigated. Also, the effect of the seismic intensity level and the gravity-only members on the fundamental period of building structures needs to be evaluated.

## References

ASCE 7-10 (2010), *Minimum Design Loads for Buildings and Other Structures* (*ASCE/SEI 7–10*), American Society of Civil Engineers, Reston, VA, USA.

COSMOS (2017), *The Consortium of Organizations for Strong-Motion Observation Systems*, http: //www.cosmos-eq.org/.

Durucan C and Gümüş M (2018), "Direct Use of Peak Ground Motion Parameters for the Estimation of Inelastic Displacement Ratio of SDOF Systems Subjected to Repeated Far Fault Ground Motions," *Earthquake Engineering and Engineering Vibration*,

**17**(4): 771–785. https://doi.org/10.1007/s11803-018-0475-4.

ECP-201 (2012), *Egyptian Code for Calculating Loads and Forces in Structural Work and Masonry*, Housing and Building National Research Center, Ministry of Housing, Utilities and Urban Planning, Cairo.

Euro code 8 (2004), *Design of Structures for Earthquake Resistance, part 1: General Rules, Seismic Actions, and Rules for Buildings, EN 1998-1*, European Committee for Standardization, Brussels, Belgium.

FEMA (2009), *Quantification of Building Seismic Performance Factors, FEMA P695*, Prepared by the Applied Technology Council for the Federal Emergency Management Agency, Washington, D.C.

Iervolino I, Galasso C, Cosenza E (2010), "REXEL: Computer Aided Record Selection for Code-Based Seismic Structural Analysis," *Bulletin of Earthquake Engineering*, **8**: 339–362. Available at: http://www.reluis.it/index.php.

Kuşyılmaz A and Topkaya C (2015), "Displacement Amplification Factors for Steel Eccentrically Braced Frames," *Earthquake Engineering & Structural Dynamics*, **44**: 167-184.

Mahmoudi M and Zaree M (2013), "Evaluating the Displacement Amplification Factors of Concentrically Braced Steel Frames," *International Journal of Advanced Structural Engineering*, **5**(13): 12.

Miranda E and Bertero VV (1994), "Evaluation of Strength Reduction Factors for Earthquake Resistant Design," *Earthquake Spectra*, **10**(2): 357–379.

Miranda E (2001), "Estimation of Inelastic Deformation Demands of SDOF Systems," *Journal of Structural Engineering, ASCE*, **127**: 1005–1012.

NBCC (2010), *National Building Code of Canada. National Research Council of Canada*, Ottawa, Ontario, Canada.

Samimifar M, Oskouei AV and Rofooei FR (2015), "Deflection Amplification Factor for Estimating Seismic Lateral Deformations of RC Frames," *Earthq Eng & Eng Vib*, **14**: 373–384.

SeismoStruct v7.0 (2014), *A Computer Program for Static and Dynamic Nonlinear Analysis of Framed structures*, available from http://www.seismosoft.com.

Uang CM and Maarouf A (1994), "Deflection Amplification Factor for Seismic Design Provisions," *Journal of Structural Engineering*, **120**(8): 2423–2436.

Veletsos AS and Newmark NM (1960), "Effect of Inelastic Behavior on the Response of Simple Systems to Earthquake Motions," *Proc. 2nd World Conf. Earthquake Eng.*, Tokyo, Japan, 2: 895–912.

Zhai C, Li S, Xie L and Sun Y (2007), "Study on Inelastic Displacement Ratio Spectra for Near-Fault Pulse-Type Ground Motions," *Earthquake Engineering and Engineering Vibration*, **6**(4): 351–355. https://doi.org/ 10.1007/s11803-007-0755-x.